Signal Processing Implementation with Microwave Photonics

Ankita Panda [1], Mitali Samal [2], Manasi Patro [3], Subrat Kumar Chand [4], Pradeep Kumar Mishra [5]
SUNIL KUMAR BISOI[6]
[1, 2, 3, 4, 5] Gandhi Institute for Education & Technology, Baniatangi, Khordha, Odisha
[6]NM Institute of Engineering & Technology,Bhubaneswar,Odisha
ankitapanda@giet.edu.in, mitalisamal@giet.edu.in, manasipatra@giet.edu.in,
subratkumarchand@giet.edu.in, pradeepkumarmishra@giet.edu.in

***Abstract*—This paper reviews the recent advances in the field of radio frequency signal processing using photonic devices and subsystems or microwave photonic (MWP) signal processing. We focus our attention on the results reported during the last six years, as previous work has been adequately addressed in previous review papers. After a brief introduction to the basic concepts involved in MWP signal processing, we focus our attention on the most significant advances reported by different research groups in overcoming their main limitation factors. Recent advances in the emergent topic of integrated MWP signal processors are also covered and the novel approaches toward the evaluation of the main figures of merit are discussed. New proposed applications and future directions of work are also considered.**

***Index Terms*—Microwave photonics (MWP), signal processing, radio over fiber.**

I. Introduction

MICROWAVE PHOTONICS (MWP) enables the transmission and processing of radio frequency (RF) signals with unprecedented features as compared to other approaches based on traditional microwave technologies [1]–[3]. An MWP signal processor is a photonic subsystem designed with the aim of carrying equivalent tasks to those of an ordinary microwave filter within an RF system or link, bringing supplementary advantages inherent to photonics such as low loss, high bandwidth, immunity to electromagnetic interference, and also providing features which are very difficult or even impossible to achieve with traditional technologies, such as fast tunability and reconfigurability.

A considerable amount of work has been carried out within the field of MWP signal processing as it is instrumental for the implementation of many functionalities including filtering, arbitrary waveform generation, optical beam-steering, analog-to-digital conversion and, more recently, frequency measurement.

The interested reader can find very detailed descriptions of the advantages as compared to traditional microwave filtering technologies, fundamental principles, limitations, and rele- vant progress reached within the field up to 2005 in several review papers [4]–[6]. Since then, relevant work and progress have been carried out in four main areas: 1) addressing and overcoming several important limitations; 2) the integration of MWP filters on a chipset; 3) development of measurement techniques; and 4) expanding their range of applications.

The purpose of this paper is to describe the most significant advances achieved within these four areas during the last six-seven years. After a brief refreshment of the basic concepts of MWP signal processing carried in Section II, we devote a specific and independent section to each of these four research areas. Section III reports the work on addressing and overcoming the most important limitations that restrict the operation of MWP filters. Section IV describes the salient work on the emergent area of filter integration, while the efforts on the characterization of MWP filters by the so-called figures of merit are reported in Section V.

A comprehensive treatment of novel reported applications of MWP signal processors is presented in Section VI. Finally, this paper is summarized and future directions pointed in Section VII.

For the sake of completeness, a reference list with over 100 papers published since 2005 is provided that supplements the more than 200 references already included in former review papers [4]–[6].

I. Basic Concepts on MWP Signal Processing

Fig. 1 illustrates the basic operating principles of an MWP signal processor. The starting point is an input RF signal with spectrum sidebands centered at frequency $\pm f_{RF}$, as shown in point 1. This signal which can have its origin either from an RF generator or from the detection by means of a single or an array of antennas modulates the output of an optical source to upconvert its spectrum to the optical region of the spectrum (point 2), such that the sidebands are now centered at $\nu \pm f_{RF}$, where ν represents the central frequency of the optical source. The combined optical signal is then processed by an optical system composed of several photonic devices and characterized by an overall lumped optical field transfer function $H(\nu)$. The mission of the optical system is to modify the spectral characteristics of the sidebands, so at its output, they are modified according to a specified requirement as illustrated in point 3. Finally, an optical detector is employed to downconvert the processed sidebands again to the RF part of the spectrum by suitable beating with

ISSN: 2278-4632
Vol-12 Issue-07 No.03 July 2022

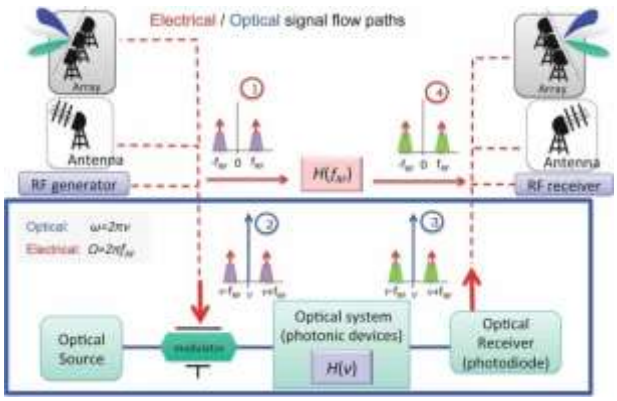

Fig. 1. General layout and operating principle of an MWP signal processor.

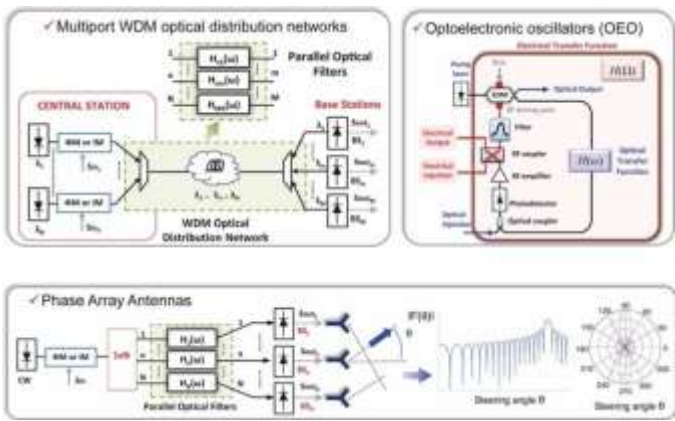

Fig. 2. Various examples of MWP signal processors in the context of different application scenarios.

the optical carrier so the recovered RF signal, now processed (as shown in point 4), is ready to be sent to an RF receiver or to be reradiated. The overall electrical transfer function $H(f_{\mathrm{RF}})$ is also shown and must not be confused with the optical field transfer function of the auxiliary optical system.

The concept of signal processing is pervasive in MWP, as shown by some examples in Fig. 2. For instance, it appears in radio-over-fiber multipoint wavelength division multiplexing networks, where each central station source/base station detector pair defines an MWP filter. It also appears in more specialized subsystems such as optoelectronic oscillators, photonic analog-to-digital converters, arbitrary waveform generators, and frequency measurement subsystems. It is also present in optical beam-steering application, where spatial diversity defines an individual MWP filtering channel between the source and each radiating element. For each particular application, a different spectral configuration is required, but the underlying concept remains the same.

The most versatile approach toward the implementation of MWP filters is based on discrete-time signal processing [4], where a number of weighted and delayed samples of the RF signal to be processed are produced in the optical domain and combined upon detection. In particular, finite impulse response (FIR) [7] filters combine at their output a finite set of delayed and weighted replicas or taps of the input optical signal, while

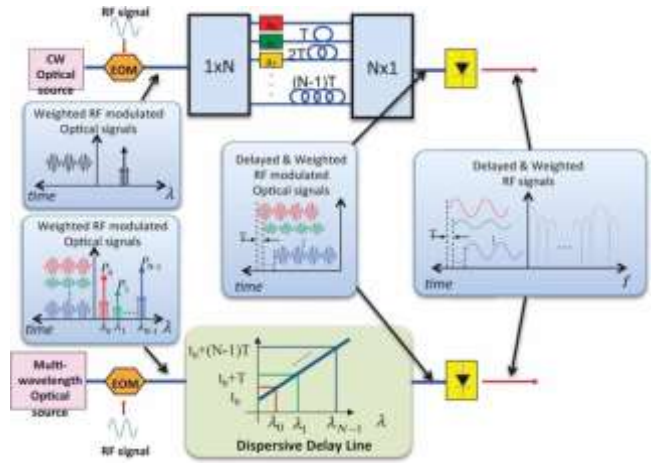

Fig. 3. General scheme of a discrete-time FIR MWP. (a) Traditional approach based on a single optical source in combination with multiple delay lines. (b) More compact approach based on a multiwavelength optical source combined with a single dispersive element.

infinite impulse response (IIR) filters [7] are based on recirculating cavities to provide an infinite number of weighted and delayed replicas of the input optical signal. For instance, and taking as an example an FIR configuration, the electronic transfer function is given by

$$H(f_{\mathrm{RF}}) = \sum_{k=0}^{N-1} a_k e^{-j2\pi k f_{\mathrm{RF}} T} = \sum_{k=0}^{N-1} |a_k| e^{jk\varphi} e^{-j2\pi k f_{\mathrm{RF}} T} \quad (1)$$

where $a_k = |a_k| e^{jk\varphi}$ represents the weight of the kth sample, and T is the time delay between consecutive samples. Note that (1) implies that the filter is periodic in the frequency domain. The period, known as the free spectral range (FSR), is given by $\mathrm{FSR} = 1/T$. The usual implementation of this concept in the context of MWP can follow two approaches, as shown in Fig. 3. In the first one [see Fig. 3(a)], the delays between consecutive samples are obtained, for instance, by means of a set of N optical fibers or waveguides where the length of the fiber/waveguide in the kth tap is $c(k-1)T/n$, being c and n the light velocity in the vacuum and the refractive index, respectively. This simple scheme does not allow tuning, as this would require changing the value of T. An alternative approach [see Fig. 3(b)] is based on the combination of a dispersive delay line and different optical carriers where the value of the basic delay T is changed by tuning the wavelength separation among the carriers, thereby allowing tunability [5], [6]. While in the first case the weight of the kth tap can be changed by inserting loss/gain devices in the fiber coils, the second approach allows to readily adjust a_k by changing the optical power emitted by the optical sources [5].

MWP filters can operate under incoherent regime, where sample coefficients in (1) correspond to optical intensities and are thus positive or under coherent regime, where the taps in (1) can be complex-valued in general. In the first case, the basic delay is much greater than the coherence time of the optical source that feeds the filter, while in the second one, it is

ISSN: 2278-4632
Vol-12 Issue-07 No.03 July 2022

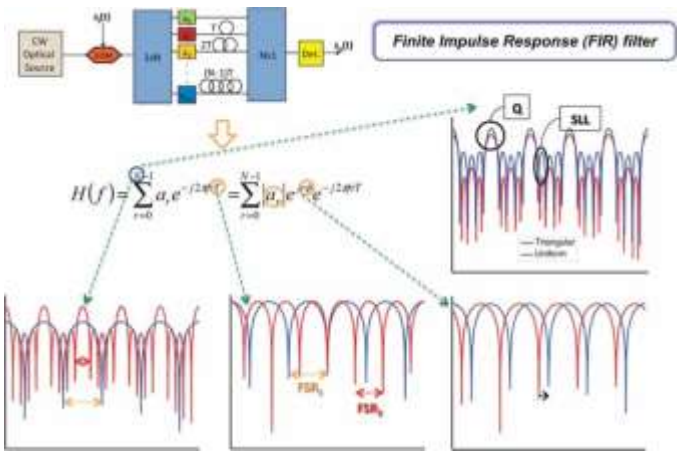

Fig. 4. Illustration of the requirements on sample parameters to achieve MWP filter tunability, reconfigurability, and selectivity.

much smaller. In practice, the overall majority of the proposed schemes work under incoherent regime as this allows the implementation of structures that are immune to environmental changes.

MWP filter flexibility in terms of tunability, reconfigurability, and selectivity is achieved by acting over the different parameters characterizing the samples in (1) with a variety of techniques previously reported in the literature [4]–[6]. The effect of the relevant parameters in (1) on the filter response is illustrated in Fig. 4.

The number of samples dictates whether the filter is either a notch $(N = 2)$ or a bandpass $(N > 2)$ type. As mentioned above, T fixes the spectral period; thus, changing T results in compressing or stretching the spectral response. This is a technique usually employed in the literature for tuning the notch or bandpass positions of an MWP filter. Fast tuning can be achieved by changing the wavelength separation between adjacent carriers in the scheme of Fig. 3(b). The phase of the tap coefficients allows the tuning of the spectral response without actually stretching or compressing it. The implementation of phase values depends on the technical approach that is followed. For incoherent MWP filters, a photonic RF-phase shifter is required which can be implemented in a variety of technologies, including stimulated Brillouin scattering (SBS), coherent population oscillations in semiconductor optical amplifier (SOA) devices and passive configurations based on ring cavities and resonators. All of the above can provide the required phase-shift dynamic range. For coherent filters, the phase shifts are optically provided by photonic components.

The law followed by the tap coefficient moduli dictates the filter shape (reconfiguration). Filters featuring different windowing functions, both static and dynamically reconfigurable structures, have been reported in the literature where tap amplitude setting has been achieved using different techniques, including spatial light modulators (SLMs), SOAs, and also by fixing the output power of laser modes.

Finally, the filter selectivity is dictated by the number of samples that determine the quality factor Q and the main to secondary sidelobe (SSL) rejection ratio.

II. Overcoming Limitations

A. Positive Coefficient and Tunability Restrictions

Photonic-assisted RF filtering schemes based on incoherent regime implementing positive coefficients show important inherent restrictions in terms of response shape and tunability [5]. In particular, tunability has been usually achieved by adjusting the basic time delay, which is inevitably accompanied by a change in the entire spectral shape [5]. However, a fine control of the center frequency of the pass-or stopband while keeping the spectral shape unchanged is highly desirable for many applications [4]. In this context, the implementation of complex-valued coefficients provides a suitable solution for overcoming this limitation. To this end, broadband and continuously tunable MWP phase shifters are of key importance.

In the past years, several technology platforms and methods have been successfully demonstrated aiming at implementing complex-valued coefficients, including those based on slow and fast light (SFL) [8] propagation in optical fibers [9]–[17], dispersion-induced effects fiber Bragg gratings [18], nonuniformly spaced delay lines [19], SFL effects in semiconductor waveguides [20]–[25], multiple electro-optic modulators (EOMs) in combination with a dispersive medium [27], 2-D liquid crystal on silicon (2D LCoS) [28] and optical frequency comb shaping [28].

SFL propagation refers to the control of the speed of light in certain media [8]. In recent years, the potential applicability of SFL effects in the implementation of MWP processing tasks has been intensively investigated using different materials and techniques. Indeed, SFL techniques employing optical fibers at room temperature, such as SBS, have been drawing particular attention since optical signals can be processed directly in the optical fiber that is used as the transmission medium SBS induces gain/loss resonances whose frequency dependence of the signal optical phase delay is nearly linear, thus providing an effective group delay [9]. Therefore, SFL propagation depends on the sign of the added group delay. The extent of the delay is continuously variable by changing the optical pump power. The narrow-band characteristics of SBS and the low optical power needed for the onset of this nonlinear effect are highly attractive for the processing of microwave signals. In this context, SBS signal processing and optical single-sideband (OSSB) modulation have been combined to perform a photonic phase shifter [10]. Two pump waves generate simultaneously Brillouin gain and loss spectra that modify the optical carrier. The OSSB modulation provides a mapping between the optical and the electrical domains. Relevant features include full 360 tuning range through an external electrical control and bandwidth only limited by the transmitters and receivers deployed. The same technique has been utilized to implement incoherent MWP filters with tunable complex-valued coefficients [11], [12]. A simple notch-type filter, whose spectral response can be tuned over an FSR without changing the filter basic delay, has been demonstrated in [11]. The filter layout, modulated signal structure, and measured tunability of the spectral transfer function are shown in Fig. 5. Note that the frequency response shape remains unaltered as the notch position is tuned.

ISSN: 2278-4632
Vol-12 Issue-07 No.03 July 2022

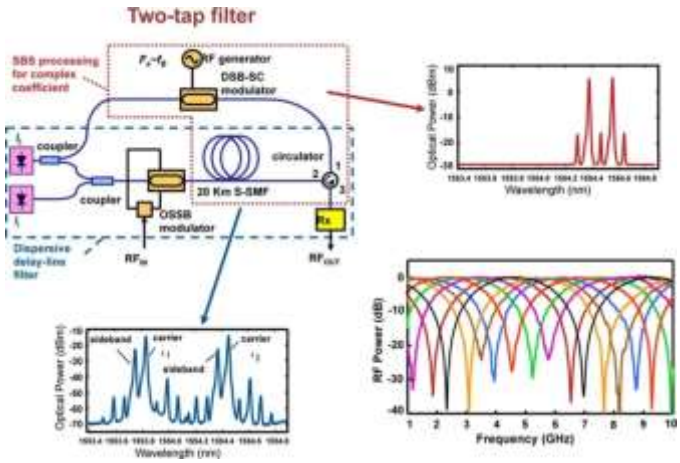

Fig. 5. Two tap notch-type MWP filter featuring complex valued coefficients implemented by means of SBS. After [11]. (Upper left) Filter Layout. (Upper right) Pumping signal to control the phase shift of the optical carrier emitting at f_2. (Lower left) RF modulated taps. (Lower right) Notch-type transfer function where the notch position is controlled the frequency value f_{RF} of the RF generator.

In addition, a multitap MWP filter approach comprising six complex-valued coefficients has been reported in [12]. It is composed of a multiwavelength source and its frequency response has been shown to be continuously tunable within an FSR/5 range, limited by the available Stokes and pump power. On the other hand, the use of slow light-induced tunable true time delay for the realization of microwave filters has been limited since the product between the maximum achievable group delay and the signal bandwidth is essentially constant. Thus, only modest group delays can be achieved for broadband baseband signals. A theoretical solution was proposed to overcome this limitation known as the separate carrier tuning (SCT) technique [13]. The SCT technique predicts that significant improvement for the generation of TTDs can be achieved by separately performing an MWP phase shifter for the carrier and the RF sideband. The above principle was experimentally demonstrated for the first time by means of SBS processing [14], [15]. In [14], a two-tap MWP filter was implemented in which the phase of a single-sideband signal was modified using SBS and that of the optical carrier was adjusted with a fiber Bragg grating. The work was later extended to implement a 100 MHz wide SBS slow light delay across a sideband that was centered at 6 GHz [15]. In this contribution, the carrier phase was adjusted through a second SBS process. The SBS-based SCT technique allowed the implementation of a reconfigurable MWP notch filter. The tunable TTD induced allowed a 20% tunability of the FSR of the filter, and the optical carrier phase shifting enabled to control the origin of the FSR variation, matching the reference frequency.

The above demonstrations require additional devices to generate the optical waves involved and rather high optical powers to pump the nonlinear interaction. On the other hand, no significant impact is produced in the noise figure as the Brillouin amplification bandwidth is very narrow. In [18], an alternative technique was introduced to obtain multitap complex-coefficient filters, which avoids the inherent complexities of using SBS processing. The technique is based on optically processing OSSB modulated signals and linear optical filtering instead of a nonlinear optical effect. The cascade of phase-shifted fiber Bragg gratings is employed for the implementation of a four-tap MWP filter. By detuning the laser wavelengths, a continuously tuning range of the filter of approximately FSR/4.36 can be obtained.

An overview of the design and implementation of complex-valued MWP FIR filters with nonuniform sampling is presented in [19]. An arbitrary bandpass frequency response was demonstrated with all-positive tap coefficients. The results showed that the FIR filters having all-positive coefficients with nonuniformly spaced taps can achieve equivalently the functionalities that require negative or complex tap coefficients. Using this concept, a 50-tap bandpass filter with a flat top and a quadratic phase response was designed and analyzed. In addition, a seven-tap nonuniformly spaced photonic microwave filter with a flat top and chirp-free bandpass response was experimentally demonstrated. The key significance of this technique is that a nonuniformly spaced FIR filter can be used to perform advanced microwave signal processing.

Among others, the semiconductor waveguide has emerged as one of the preferred technologies for the implementation of MWP phase shifters due to its performance, maturity, the possibility of both electrical and optical control and ease of integration [20]. The demonstration of MWP true-time delay lines [21] and phase shifters [22]–[24] has been performed using SOA-based schemes. In particular, the cascade of functional blocks, which are composed of an SOA followed by an optical notch filter (ONF) [22], [23], has been presented by Xue *et al.* as a suitable solution for implementing fully and continuously tunable MWP phase shifters operating at bandwidths comprising from few to several over 40 GHz [24], as illustrated in Fig. 6. Tunability ranges exceeding 2π radians for phase shifters have been demonstrated, leading to the implementation of filtering schemes involving fully adjustable complex-valued coefficients. This fact enables the achievement of tuning ranges over the filter FSR greater than 100%. The main drawback, however, stems from the system complexity since five SOAs and three ONFs are required [24]. Furthermore, a typical noise figure degradation of 10 dB is observed despite the fact that optical filtering is performed after each amplification stage. To overcome these limitations, a customized approach involving a single SOA followed by a tailored ONF, which accurately exploits the combination of both slow and fast light effects, has been recently demonstrated in order to implement a fully and continuously tunable MWP phase shifter [25]. This configuration has been employed to implement a complex-valued coefficient based MWP filter [26]. In this case, 2π phase shifts have been accomplished in combination with the phase inversion phenomenon that can occur in the EOMs [26]. These two novel approaches pave the way toward the implementation of SOA-based complex-valued coefficients with low complexity and reduced power consumption.

A parallel-connected tandem composed of two EOMs, which are modulated by the in-phase and the quadrature components of the RF signal, has been proposed and experimentally demonstrated for the implementation of complex-valued coefficients as well [27]. The scheme enables fully 2π phase shift tunability by simply adjusting the bias voltages applied to both EOMs.

ISSN: 2278-4632
Vol-12 Issue-07 No.03 July 2022

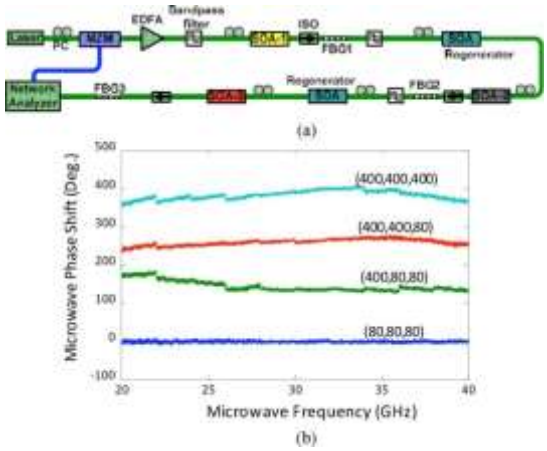

Fig. 6. (a) Microwave phase shifter based on three cascaded SOA-based phase shifter stages. (b) Measured microwave phase shift as a function of the modulation frequency for different SOA injection currents [24].

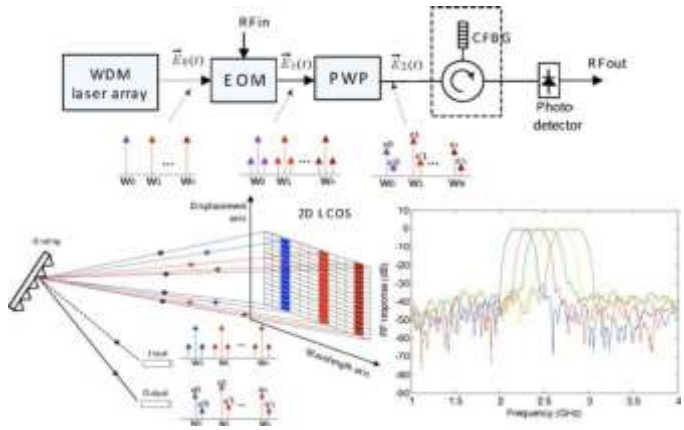

Fig. 7. MWP filter featuring multiple and independent complex valued coefficients using a 2-D liquid crystal (LCoS)-based programmable wavelength processor (PWP), after [28]. (Upper) Filter layout. (Lower left) 2-D LCoS PWP and (Lower right) measurement of tunable bandpass.

The phase shifter bandwidth is limited by the EOMs spectral response, leading to broadband phase shifts over several tens of gigahertz [27].

Researchers from University of Sydney have been recently presented a novel MWP signal processor based on 2-D array of liquid crystal (LCoS) pixels [28], which is shown in Fig. 7. Complex-valued coefficients are obtained for each wavelength in the following way. First a single sideband modulation operation is performed over the optical carrier. In a second stage, the optical carrier and the selected sideband are directed, by means of a spatial grating to two different pixels of the LCoS array where they can be independently modulated in amplitude and phase. Upon beating at the photodetector, a complex valued coefficient is obtained, where the amplitude is the product of the amplitude of the optical carrier and the subcarrier while the phase is the difference between the phases of the optical carrier and the sideband [28]. Consequently, arbitrary programmable complex-valued multitap filters leading to shape-invariant tuning over the full FSR can be implemented [28]. Impressive performance in terms of operating bandwidth has been demonstrated provided by the wavelength independent behavior of the LCoS structure. Moreover, tunability is achieved by simply programming each pixel of the 2-D array, without changing the rest of the approach configuration [28].

The use of a frequency comb as a light source in combination with an interferometric scheme has been recently proposed and demonstrated in the implementation of MWP filters with complex-valued coefficients by researchers from Purdue University [29]. Complex programmability of a considerable number of taps generated by the frequency comb has been achieved by line-by-line pulse shaping using a novel interferometric scheme [29]. Tunability has been performed by an extremely fine chirp control in the interferometric structure, leading to precise tunings. In contrast, the operating spectral region is limited by the frequency detuning between adjacent samples.

A particular case of complex-valued coefficients is negative coefficients, which are generated by imprinting a π phase shift (phase inversion) on a positive coefficient. The implementation of advance filtering schemes involving negative coefficients leads to unique spectral features. In particular, baseband free filter frequency responses can be performed. This fact allows avoiding the undesired crosstalk caused by the dc and low-frequency contributions in certain applications. Different techniques have been successfully demonstrated for implementing negative coefficients in the past few years, mainly based on exploiting phase-to-intensity modulation (PM-IM) conversion [30]–[32], using polarization modulators (PolM) [33], [34] and cladding-mode couplers [35].

By propagating the phase-modulated optical carriers implementing the filter coefficients through a dispersive medium, PM-IM conversion takes place enabling the production of negative coefficients. As a dispersive medium, linearly chirped fiber Bragg gratings (LCFBG) [30] and fiber loops [31] have been traditionally used. A more flexible approach based on single sideband selection has been proposed by Mora *et al.*, which allows for the generation of arbitrary positive or negative coefficients without altering the dispersion feature and the polarization bias of the modulator [32]. Since phase modulation naturally produces an upper and a lower modulation sideband with a π phase shift the technique is based on selecting, after the phase modulation stage the carrier and the upper or the lower sideband depending on whether a positive or negative coefficient is to be implemented by that particular wavelength. This selection is performed by means of optical filtering. The coefficient sign is obtained upon beating of the selected subcarrier and the optical carrier in the photodetector.

The use of PolMs together with polarization-maintaining fibers (PMF) has been also identified as advantageous in the implementation of negative coefficients. The basic concept relies on adjusting the polarization status of the incident light wave into the PolM to be aligned at an angle of 45° with respect to the principal axes [33], as illustrated in Fig. 8. In this way, two complementary optical microwave signals are generated, which are polarization-dependent delayed by the PMF. The extrapolation of this technique to any number of coefficients, as well as to the implementation of arbitrary positive and negative

ISSN: 2278-4632
Vol-12 Issue-07 No.03 July 2022

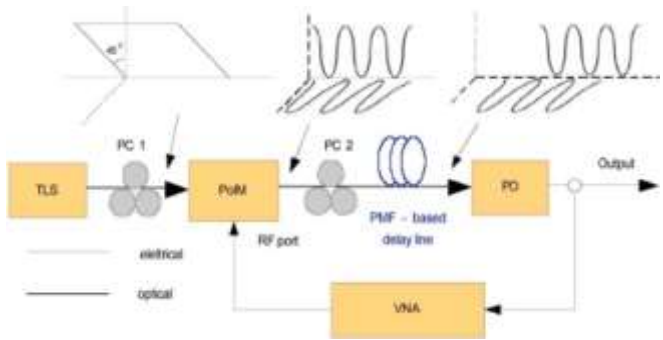

Fig. 8. Schematic diagram of a photonic microwave bandpass filter with negative coefficients based on polarization modulation in an electro-optic polarization modulator [33]. TLS: tunable lightwave source, VNA: vector network analyzer.

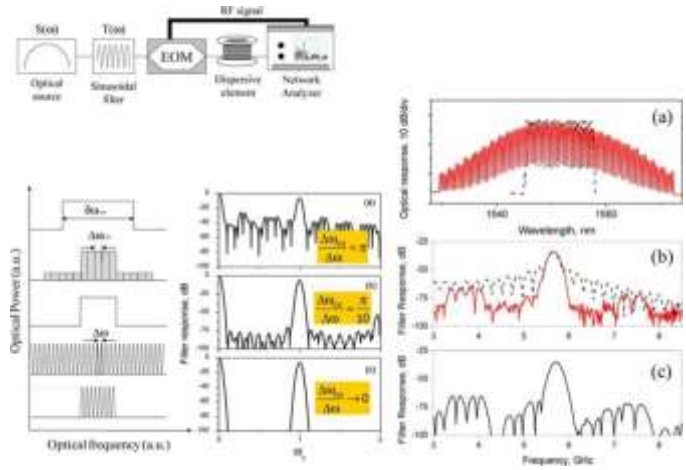

Fig. 9. (Left) layout and operating principle of the single resonance filter obtained by spectral sinusoidal sampling [39], [40]. (Right) Experimental versus theoretical results for uniform and Gaussian apodization of the broadband source. (a) Shaped spectrum of the optical source (uniform and Gaussian). (b) Measured responses for the MWP filters using a uniform and Gaussian shaped input source. (c) Theoretical response for the MWP filter using a Gaussian-shaped input source.

coefficients have been also proposed and demonstrated in [33] and [34], respectively.

Negative coefficients deploying cladding-mode couplers in combination with optical injection locking of a large wavelength detuning have also been demonstrated [35]. In this case, the phase inversion results from optical injection locking of a single-mode laser, whereas continuous tunability is realized by physically sliding a pair of bare fibers inside the cladding-mode coupler [35]. Large extinction ratio and tuning ranges have been verified [35].

B. Spectral Periodicity Restrictions

The overall majority of the proposed MWP filtering structures display a periodic transfer function (as sketched in Fig. 4), which is a consequence of their discrete time nature. While spectral periodicity can be advantageously employed for certain applications, in most cases, it imposes a limitation since it can add crosstalk from undesired RF bands. To overcome this limitation, several techniques [39]–[45] which can help either to expand the spectral period or even achieve single resonance responses have been actively researched over the last years.

One interesting option reported in [39] and [40] is to use sinusoidal sampling of a spectrally shaped broadband optical source. This process consists in essence in multiplying the spectrum broadband source shaped with a spectral resolution of $\Delta\omega_{CH}$ by a sinusoidal spectrum (with period $\Delta\omega_{CH}$) provided by an optical filter. If $\Delta\omega/\Delta\omega_{CH}$ is small enough, the overall effect is similar to a sampling by a train of delta functions with the difference that the sampling signal does not reach the zero value. This results in a semi-discrete time filter which eliminates spectral periodicity so only two resonances (one at baseband which can be blocked) and another at the frequency of interest are generated. The resonance position is controlled by the spectral period of the sinusoidal sampler $\Delta\omega$, while the peak to SSL ratio is given by $\Delta\omega_{CH}/\Delta\omega$. The left part of Fig. 9 shows a layout of this structure and illustrates the basic operating principle while the right part provides experimental versus theoretical results obtained when a squared and a Gaussian source apodization is applied in the spectral conformation of the broadband optical source. A second alternative recently proposed [41] combines the use of discrete-time bipolar taps to eliminate the baseband response with the convolution of the filter time domain samples with pulses featuring a low-pass spectrum with a bandwidth that overlaps only one resonance of the discrete-time filter.

The use of filter cascades to select a single resonance has been theoretically analyzed in [42], where conditions to achieve linearity in the RF domain have been derived as, in general, linearity is only guaranteed in the optical domain. Several experimental configurations based on these filter cascades using ring resonators (RRs) and fiber Bragg gratings have been reported in [43] and [44].

In [45], an interesting technique is reported based on SBS, which is shown in Fig. 10. Using the complementary amplitude responses (gain or loss) provided by two Stokes and anti-Stokes pumping carriers, equally spaced from a RF-phase-modulated optical carrier, one can eliminate one of the sidebands for a specific RF frequency, hence turning an initially destructive interference into constructive (bandpass) within a very narrow spectral region around the RF sideband. The position of the constructive interference can be continuously tuned by changing the wavelengths of the pumping signals. Tuning ranges in excess of 20 GHz with Q factors of 1000 have been reported using this technique.

C. Coherence Limitations

Although, as previously mentioned, the main operation regime of MWP filters is based on using incoherent sources, several works [45]–[50] have reported and experimentally demonstrated that it is possible to overcome the limitations that source coherence imposes over the operation of MWP filters. The use of coherent laser sources is interesting as higher input powers can be injected into the filter thus reducing the RF link losses. In the context of MWP filtering, a coherent source is that having a coherence time (i.e., inverse of its linewidth) much longer that the basic delay T between adjacent samples. If such sources are employed, then optical interference due to mechanical and environmental fluctuations can severely compromise the filter performance. An interesting technique is based on

ISSN: 2278-4632
Vol-12 Issue-07 No.03 July 2022

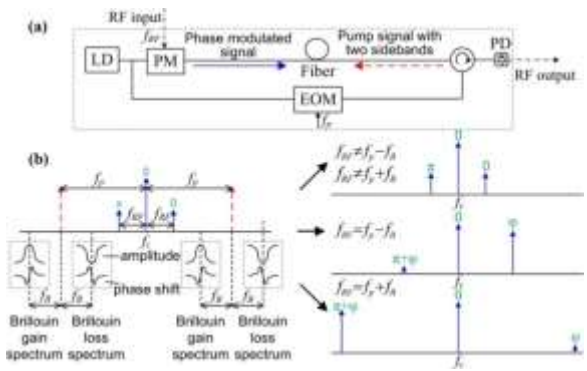

Fig. 10. (a) layout, (b) operating principle, and (c) experimental results of the single resonance filter obtained by controlled interference using SBS.

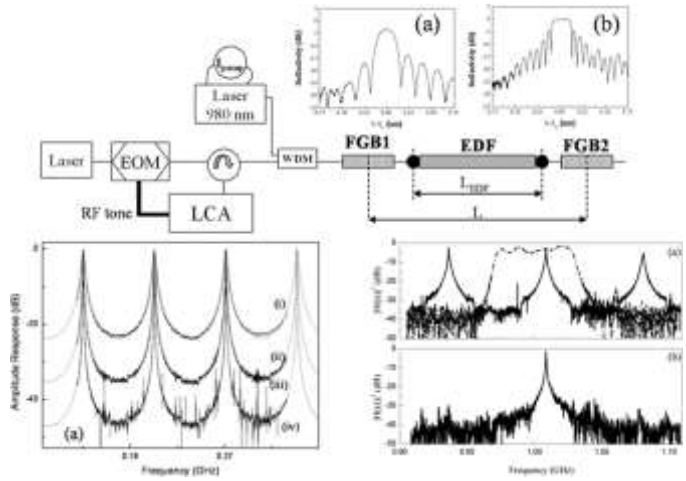

Fig. 11. Ultraselective bandpass MWP filter using an IIR structure and a tuned modulator, after [53]. (Upper part) Filter layout. (Lower left part) Transfer function using a broadband EOM. (Lower right part) Transfer function using a tuned modulator.

controlling the source coherence by means of the application of an external phase modulation [47]. Here, a residual phase modulation applied at the output of the optical source increases its linewidth thereby reducing its coherence time and, therefore the effects of interference. Schemes overcoming coherence limitation have been proposed for single cavity notch type [46], high-performance amplified bandpass filters [49], and complex structures based on the cascade of cavities.

D. Selectivity, Spectral Quality and Speed Restrictions

High quality (Q) factor and high contrast ratio filters are needed to efficiently select or suppress a given RF band. On the other hand, flexible and very fast reconfigurability allows the rapid change of a filter transfer function for dynamic and adaptive applications. In both cases, recent developments in the field of MWP filters provide a variety of techniques and approaches featuring values and figures that outperform those obtained using traditional RF techniques.

High selectivity filters have been reported both for notch and bandpass operation [51]–[54]. In [51], an ultraselective notch filter is reported which is implemented by feeding two different lasers (emitting at λ_1 and λ_2, respectively) modulated in counterphase by the same RF signal to an amplified recirculating delay line which contains a wavelength filter to block the λ_2 component. Thus, the structure implements a bandpass filter for the λ_1 component and an all-pass characteristic for the λ_2 component. These are subtracted upon beating in the photodetector. The substraction of the bandpass characteristic (obtained for λ_1) from the all-pass response (obtained for λ_2) features a high resolution notch response with a notch width of 0.55% of the filter FSR and a deep notch of over 40 dB depth with stable performance even though the laser sources have a narrow linewidth.

A highly selective FIR bandpass filter was proposed and experimentally demonstrated in [52] which was based on the combination of an FBG-based tapped delay line providing a spectrally periodic filter and a tuned EOM which operated in a bandpass region of the RF spectrum covering only one spectral period. The filter was designed to be tunable over the UMTS spectral band using switched dispersive delay lines and featured a quality factor of 234. Much higher quality factors for bandpass filters were subsequently reported using an amplified IIR structure combined with a tuned modulator [53], [54]. A Q factor in excess of 3000 was reported in [53] using the configuration shown in Fig. 11.

An amplified IIR filter was assembled by embedding a piece of erbium-doped fiber (EDF) between two FBG devices. The EDF was optically pumped to produce the required cavity gain to sustain the sample amplitudes without reaching laser oscillations. The IIR structure was fed by an RF modulated CW laser. Using a broadband external modulator resulted in a typical periodic filter, where the resonance bandwidth could be controlled, by a precise setting of the optical pump signal, as shown in the lower left part of Fig. 11. Single resonance operation was achieved by substituting the broadband external modulator by a tuned device.

Significant progress on spectral quality and programmable filter transfer function reconfigurability has been achieved by spectral shaping of optical broadband [55] and comb sources [56]–[60]. In the first case [55], shown in the upper part of Fig. 12, a broadband optical source was shaped in amplitude by means of a diffraction grating which spatially separated 40 wavelength components (0.8 nm channel separation). Each one was sent to a different programmable SLM to shape its amplitude. All of them were subsequently combined and fed into one of the two inputs of an external modulator by means of an optical switch (depending on the positive or negative sign of the coefficient to be implemented) to inject the RF signal to be processed. A dispersive fiber link placed after the modulator provided the required frequency to time mapping prior to photodetection. Changing the wavelength amplitudes through a controlling computer allowed the dynamic shaping of the transfer function featuring different windowing functions. The lower part of Fig. 12 displays theoretically expected and measured results of different transfer functions corresponding to a diverse windowing or apodization functions currently employed in signal processing applications.

The former scheme is quite flexible but in principle does not allow filter tunability. However, a similar scheme based on optical comb sources [56]–[60] overcomes this limitation

ISSN: 2278-4632
Vol-12 Issue-07 No.03 July 2022

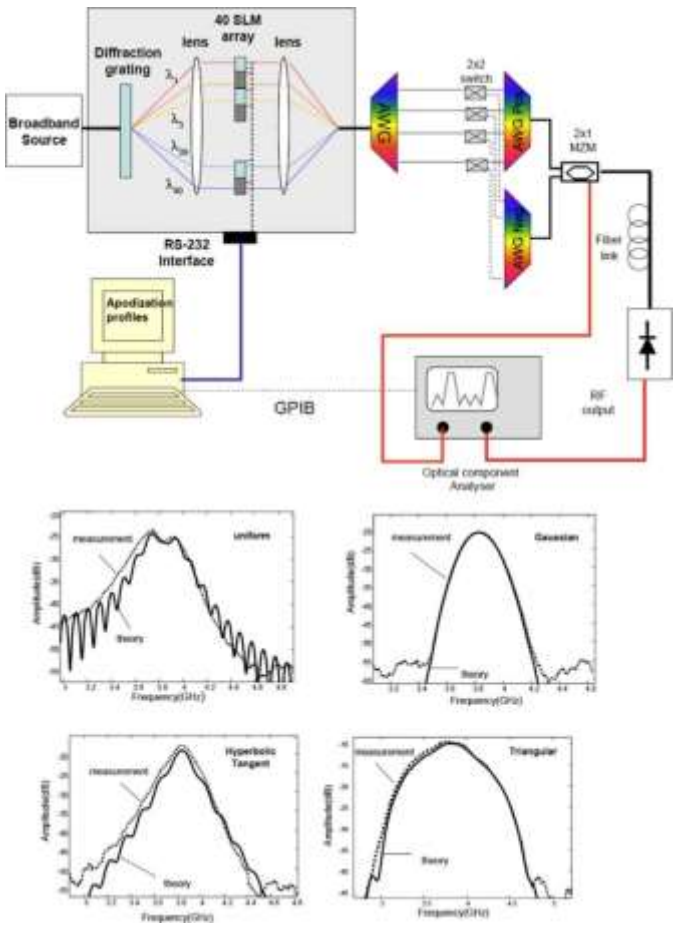

Fig. 12. Dynamically reconfigurable MWP filter based on the spectral amplitude shaping of a broadband optical source. (Upper) Layout of a processor featuring positive and negative coefficients. (Lower) Theoretical and measured transfer functions for different windowing profiles after [55].

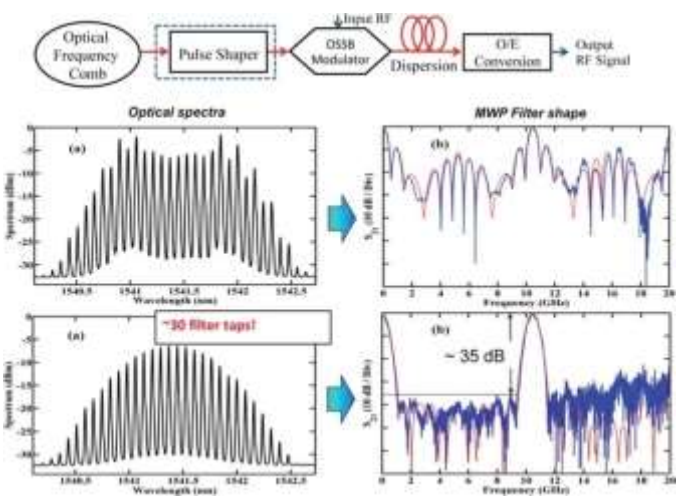

Fig. 13. Dynamically reconfigurable MWP filter based on the spectral amplitude shaping of an optical comb source. After [56].

while also providing the possibility of very fast tunability. The basic approach, proposed by researchers at Purdue University is shown in Fig. 13.

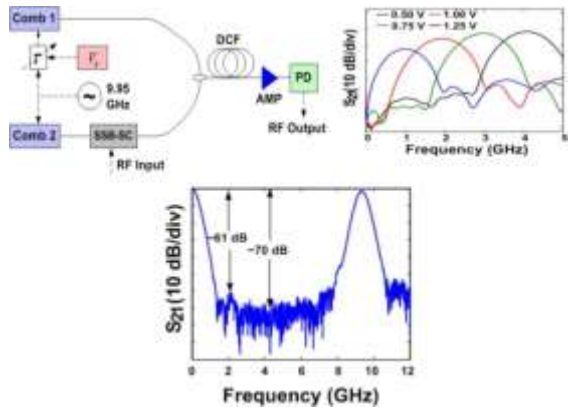

Fig. 14. (Upper left) Modified transmitter for the implementation of complex-valued tunable MWP filters based on the spectral shaping of optical Comb sources. (Upper right) Demonstration of resonance tunability by means of a voltage control signal. (Lower) Transfer function after increasing the number of samples by four wave mixing. After [59].

The operating principle is very similar to that described in the case of using a broadband optical source. The main difference is that here an optical comb source generated by laser modelocking is employed. The output modes are independently shaped providing the desired windowing functions and the conformed optical spectrum is then modulated by the RF signal and transmitted through a dispersive fiber link. The lower part of Fig. 13 provides two examples corresponding to different spectral shaping functions using a comb source featuring 30 modes and the resulting filter transfer functions. As expected by using a Gaussian windowing, the SSLs are considerably reduced (MSSL > 35 dB). One fundamental advantage of this structure is that it can be made tunable by implementing complex-valued coefficients [59]. This can be achieved by replacing the single comb source by a more elaborated transmitter employing two identical comb sources, as shown in Fig. 14.

The modes of one comb source are phase delayed with respect to their equivalents in the other. The value of the phase shift is controlled by means of a voltage signal. Phase shifted modes are not RF modulated while the modes in the other comb are RF single sideband modulated with carrier suppression.

Upon combination, each wavelength contains an optical carrier phase-shifted with respect to its sideband or, in other words, a complex-valued coefficient. The upper right part of Fig. 14 shows how by increasing the control voltage the phase shift is changed and the filter resonance position is tuned. This tuning mechanism can be extremely fast with record values of 34 ps as reported in [59]. Furthermore, the number of samples can be increased by means of exploiting nonlinear four wave mixing effects and thus increasing the MSSL. For instance, in [59], a record MSSL value of over 60 dB has been demonstrated as shown in the measured transfer function displayed in the lower part of Fig. 14.

III. Integrated MWP Filters

The possibility of integrating MWP filters in a single chip is highly attractive since this will open the way to structures with reduced footprint, lower power consumption, higher stability, and reliability. Furthermore, cost reduction due to the possibility

ISSN: 2278-4632
Vol-12 Issue-07 No.03 July 2022

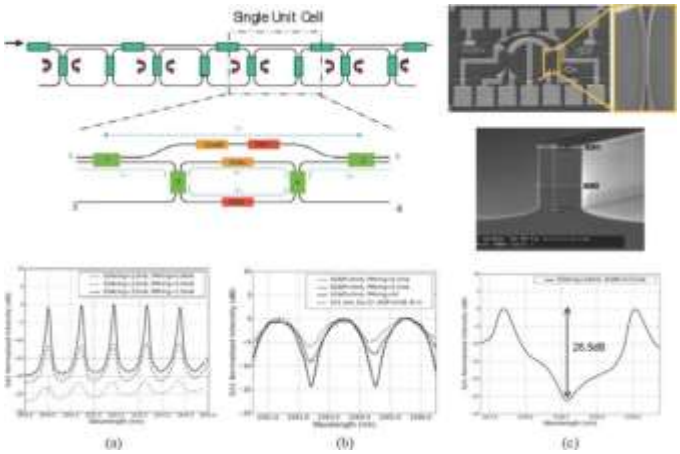

Fig. 15. Integrated InP-InGaAsP first-order MWP coherent filter providing one pole and one zero reported in [64]. (Upper) Unit cell configuration, contacts and waveguide pictures. (Lower) Measured transfer functions for one pole (left), one zero (center), and one pole-one zero (right) configurations.

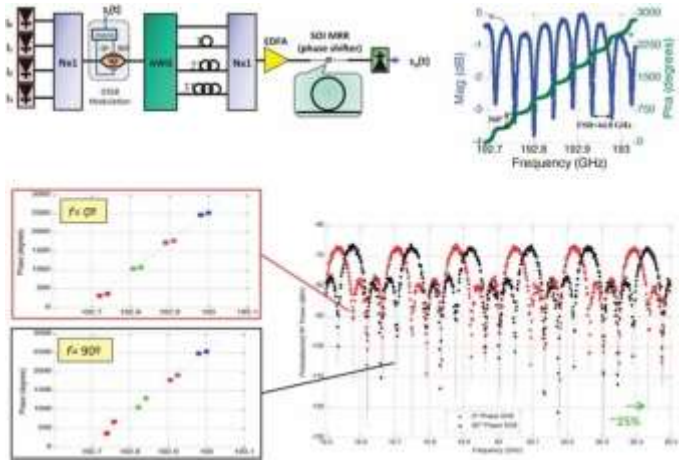

Fig. 16. Tunable incoherent MWP filter based on multiple phase shifters implemented by periodic resonances of an integrated SOI RR. (Upper left) Filter configuration. (Upper right) Amplitude and phase response of the SOI RR. (Lower left) Spectral locations of the four optical carriers and subcarriers to achieve, respectively, 0° and 90° phase shifts. (Lower right) Filter transfer functions corresponding to the two cases (0 and 90° phase shifts) showing tunability. After [72].

of mass production is another fundamental advantage. Several groups [25], [26], [61]–[78] have reported interesting results in the integration of both coherent and incoherent filters. To date, however, integration has been demonstrated only for selected parts of these subsystems.

As far as MWP coherent filtering is concerned, many of the preliminary approaches reported so far have been based mainly on single cavity RRs. A few however have also focused on more elaborated designs involving more than one cavity and programmable features. These filters can be useful particularly when the RF information has already been modulated onto the lightwave carrier and it might be advisable to perform some prefiltering in the optical domain prior to the receiver. Representative results from one cavity filters can be found in [61]–[63], [66], and [67]. For instance, Norberg *et al.* [61] report the results for a unit cell, shown in the upper of Fig. 15 that could be an element of more complex lattice filters.

This unit cell, integrated in InP-InGaAsP, is composed of two forward paths and contains one ring. By selectively biasing one SOA and phase modulators placed in the arms of the unit cell, filters with a single pole, a single zero or a combination of both can be programmed as shown in the lower part of Fig. 15. In particular and for the design reported in [65], the frequency tuning range spans around 100 GHz. A hybrid version incorporating silicon waveguides has also been reported [67], [68] that combines III–V quantum well layers bonded with low-loss passive silicon waveguides.

Low-loss waveguides allow for long loop delays while III–V quantum devices provide active tuning capability. The same group involved in [65] is now reporting results of more complex designs involving second and third order filters as well as other different unit cell configurations [66].

A more complex design, this time in Silicon, has been also recently presented in [69] and [70] where 1–2 GHz-bandwidth filters with very high extinction ratios ($\sim$ 50 dB) have been demonstrated. The silicon waveguides employed to construct these filters have propagation losses of ~ 0.5 dB/cm and insertion losses (excluding fiber to waveguide coupling) where in the range of 2–3.5 dB. Each ring of a filter is thermally controlled by metal heaters situated on the top of the ring. With a power dissipation of mW, the ring resonance can be tuned by one FSR, resulting in wavelength-tunable optical filters. Both the second-order and fifth-order RRs have been demonstrated, which can find ready application in RF/microwave signal processing.

Work on integrated MWP incoherent filters has been reported by various groups [25], [26], [72]–[78] as well. Recent efforts have focused towards the implementation of complex-valued sample filters by means of exploiting several techniques to integrate MWP phase shifters. For instance, two-tap tunable notch filter configurations where phase shifting was achieved by means of coherent population oscillations in SOA devices followed by optical filtering were reported in [25] and [26]. In another approach [72], the periodic spectrum of an integrated SOI RR is employed as a multicarrier tunable and independent phase shifter. The configuration for a four-tap filter is shown in Fig. 16.

Here, the basic differential delay between samples is implemented in the first stage, while an independent phase coefficient for each tap is selected in the RR by finely tuning the wavelength of each carrier. A similar configuration based on a hybrid InP-SOI tunable phase shifter has also been recently reported [73]. In this case, tuning is achieved not by changing the source wavelength but by carrier injection into the III–V microdisk. A more versatile configuration which can provide both phase and optical delay line (ODL) tuning has been recently reported based on the Si_4N_3 TripleX technology [74]–[76]. It consists of a reconfigurable ODL with an SCT [75] unit and an optical sideband filter on a single CMOS compatible photonic chip. The processing functionalities are carried out with optical RRs as building blocks demonstrating reconfigurable MWP filter operation in a bandwidth over 1 GHz.

Most of the incoherent MWP filters reported so far require a dispersive delay line which is usually implemented by either a dispersive fiber link or an LCFBG which being bulky devices,

ISSN: 2278-4632
Vol-12 Issue-07 No.03 July 2022

prevent a complete integration of the filter on a chip. The ultimate and most challenging limitation towards the full implementation of integrated MWP signal processors is, therefore, the availability of a dispersive delay line with a footprint compatible with the chip size. It provides at the same time the group delay variation required by high-frequency RF applications. A very attractive approach is that based on a photonic crystal (PhC) waveguide which, if suitably designed, can fulfill the above requirements introducing moderate losses. Researchers have recently demonstrated for the first time both notch and bandpass microwave filters based on such component [77]. Tuning over 0–50 GHz spectral range is demonstrated by adjusting the optical delay. The underlying technological achievement is a low-loss 1.5 mm long PhC waveguide capable of generating a controllable delay up to 70 ps still with limited signal attenuation (10 dB fiber to fiber loss) and degradation. The later allows the operation of the filter with a moderate optical input power (0 dBm) to the PhC waveguide. Owing to its very small footprint, more complex and elaborate filter functions are potentially feasible with this technology. Considerable progress is still expected in this field in the coming years by considering other nonlinear material systems and technologies as reported in [78].

IV. Figures of Merit

MWP signal processors can be considered as filtered MWP links and thus their performance evaluated in terms of three common metrics, RF gain, noise figure, and dynamic range [79]. Models have been developed recently for filtered MWP links subject to frequency [80] and amplitude/phase modulation [81]. In [81], the concept of filtered MWP Links is proposed in order to provide the most general and versatile description of complex MWP systems. In particular, a field propagation model is developed where a global optical filter, characterized by its optical transfer function, as shown in Fig. 1, embraces all the intermediate optical components in a linear link and a nonmonochromatic light source characterized by an arbitrary spectral distribution is considered. Closed expressions leading to the computation of the main figures of merit concerning the link gain, noise, and spurious free dynamic range due to intermodulation distortion are given which are useful as they directly provide performance criteria results for any kind of processor just by substituting in the overall closed-form formulas the numerical or measured optical transfer function characterizing the link. Successful testing of the model has been experimentally reported for sliced broadband source and Mach–Zehnder (MZ) interferometer continuously sampled filters [82].

V. Novel Applications

A wide variety of novel applications have been proposed during the last years where MWP signal processors can play a crucial role including, among others, ultrawideband (UWB) and arbitrary waveform generation, chirped microwave pulse generation, waveform compression, and microwave differentiators.

Numerous techniques for the generation of UWB signals have been reported [83]–[88]. UWB technology has attracted a great interest for high-capacity wireless communications, sensor networks, radar, imaging, and positioning systems due to different benefits including lower power consumption, immunity to multipath fading, the possibility of interference mitigation by means of exploiting spread spectrum techniques, carrier free, high data bit rate, and capability to penetrate through obstacles. However, UWB systems have a drawback due to their short signal transmission range, on the order of less than a few tens of meters. Here, the use of optical fiber for UWB signal distribution (known as UWB-over-fiber) has emerged as a promising solution to increase the coverage area. The need of electro-optical conversions for the transport of the signal favor the case for optically generation of UWB signal since it can profit from the inherent advantages of MWP devices and subsystems.

In this context, several techniques have been already reported for optically generating UWB pulses, which are focused towards addressing two challenges. First, an important interest is found in relation to the implementation of high-order pulses as an efficient solution to comply with the FCC mask in terms of power spectral density terms [83], [84]. Most of the techniques are focused on the generation of classical UWB pulses (monocycle and doublet) which actually do not totally comply with FCC spectral requirements. In order to increase the flexibility in the generation of UWB pulses, an *N*-tap MWP filter has been proposed using phase inversion in electro-optical modulators for obtaining positive and negative taps [83]. As shown in Fig. 17, the flexibility of the system permits to incorporate a high number of coefficients and consequently, to implement high-order pulses. Also, structures that combine optical broadband sources and interferometric structures have been proposed to implement multiband UWB signals [84].

Apart from satisfying the FCC-specific spectral mask requirements, UWB optical pulse generators face another recent key challenge which is related to the possibility of pulse encoding using different modulation techniques such as pulse position modulation, pulse polarity modulation, or biphase modulation, pulse amplitude modulation, ON–OFF keying modulation and orthogonal pulse modulation by means of using photonic procedures [85]–[88].

MWP filter configurations have also been proposed for the generation of arbitrary RF waveforms [89]–[92] which are useful in a wide variety of applications. Probably the most impressive advance in the field so far is that reported in [90] where an ultra-broad-bandwidth arbitrary RF generator based on a silicon photonic spectral shaper is presented which is capable of synthesizing burst RF waveforms with programmable time-dependent amplitude, phase and frequency.

The central frequency of the waveforms can be tuned up to 60 GHz. The generator is based on the wavelength to time conversion of the broad spectrum of a mode-locked pulsed laser which is previously shaped by a photonic integrated circuit (PIC) consisting in eight independent RRs. The original proposal employs the notch-type of the through port spectral characteristic of an RR. By independently tuning (using a heater) the notches of each RR, the broadband spectrum of the mode-locked laser output is carved and this characteristic is directly translated to the time domain using a dispersive element (fiber spool). In practice, it is much better to employ the drop port characteristics (bandpass resonances) of the RRs. Furthermore, by replacing the output couplers of the RRs by tunable MZs, the amplitude

ISSN: 2278-4632
Vol-12 Issue-07 No.03 July 2022

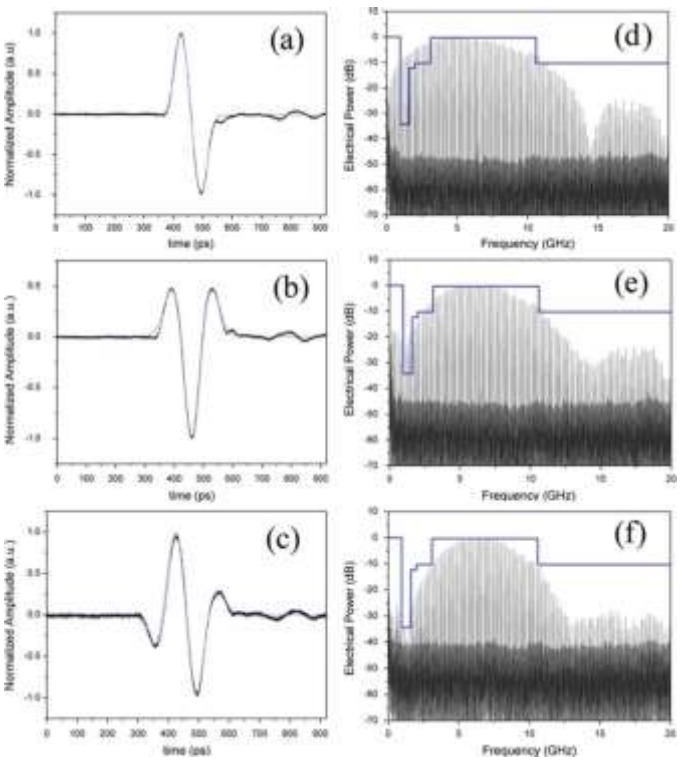

Fig. 17. Experimental (black line) and theoretical (blue line) waveforms for (a) monocycle pulse, (b) double pulse and (c) high-order pulse with 4-coefficients. In (d), (e) and (f) blue line represents the FCC mask for the corresponding experimental normalized electrical power (black line).

of the bandpass can be programmed providing full amplitude and wavelength tunability of the resonances that compose the shaped spectrum and, therefore the time characteristics of the burst signal. Some interesting figures of the chip are the following: SOI technology with a footprint of 0.1 mm× 1.2 mm, total optical loss of the PIC: 25 dB with a main contribution (10 dB) from each fiber to chip coupling interface. Tuning speed (millisecond to microsecond range). The most salient feature of this configuration is its versatility in terms of the burst shape which can be reconfigured and the output central frequency which can be easily tuned up to 60 GHz.

Another application field of interest is the photonic generation of chirped microwave pulses featuring a broad frequency operation range and high values of time-bandwidth product. Several applications benefit from these features, such as spread spectrum communications, pulsed compression radars or tomography for medical imaging [94]–[96]. We can find an approach to implementing microwave pulse compression using a photonic microwave filter with a fiber Bragg grating with a specific nonlinear phase response [94]. The key advantage of this approach is that the system can be implemented using pure fiber-optic components, which has the potential for integration. Also, chirped microwave pulses can be generated using nonuniformly spaced multiwavelength source and a length of dispersive fiber [95] and employing broadband optical sources with dispersive elements which second order dispersion is not negligible [96].

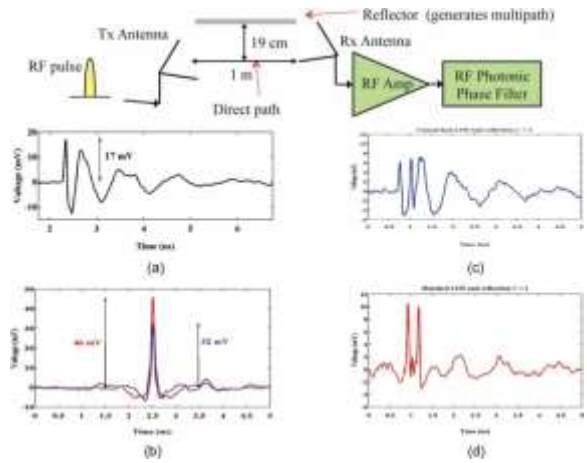

Fig. 18. (Upper) Antenna/radar link configuration followed by an RF amplifier and an MWP phase filter. (a) Output electrical waveform when the pulse shaper is quiescent. (b) Output dispersion compensated electrical waveform after the phase filter is applied, and calculated dispersion-compensated electrical waveform by an ideal photonic phase filter in solid and dashed lines, respectively. (c) Radar link response with TM reflection without the phase filter. (d) Radar link response after applying the dispersion compensating filter. After [97].

MWP signal processors have been proposed by researchers from Purdue University for the simultaneous waveform compression and dispersion post-compensation of ultrawideband antenna links [97] where, even, if the antenna gains are frequency independent, the propagation medium is dispersive. This has been achieved by using a RF photonic phase filter shown in Fig. 18. Initially, the impulse response of the antenna link was obtained using a 30 ps pulse [see Fig. 18(a)]. The dispersed RF signal detected by the antenna was then amplified by a broadband RF amplifier and then up-converted to optical frequencies using a MZ-modulator. The output of the MZ-modulator was the injected to an SLM [97]. Only the phase of the optical signals was controlled, yielding a programmable MWP phase filter that allowed the realization of any arbitrary phase response. Fig. 18(b) shows the compressed voltage pulse with duration of 65 ps full-width at half-maximum (FWHM) (blue curve). The RF peak power gain was 5.52 dB. Assuming an ideal photonic phase filter with no limitations the pulse could be compressed up to 64 ps FWHM yielding a 8.67 dB of power gain (red curve) [97].

To experimentally validate the phase filter in radar applications, two propagation paths, line-of-sight and reflection from a target, were implemented [see Fig. 18(a)]. The antennas were placed separated by about 1 m and they were tilted upwards in order to obtain two paths with equal transmission amplitude. The target was implemented using a metal plate placed 19 cm away from the line-of-sight path. The response from the two paths is displayed in Fig. 18(c). As it can be seen it was not precise enough to specify the presence of a target and its location. Fig. 18(d) shows the link response after applying the MWP phase filter. Two distinct pulses are clearly resolved, with separation of about 223 ps, which was in reasonable agreement with the calculated value [97].

A microwave bandpass differentiator is another key application recently proposed. A version based on an FIR photonic

ISSN: 2278-4632
Vol-12 Issue-07 No.03 July 2022

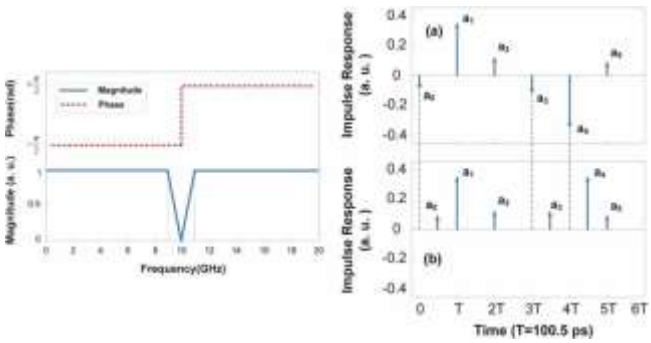

Fig. 19. (Left) Frequency response of a bandpass microwave differentiator Design of the temporal differentiator based on a six-tap FIR filter. (Upper right) Impulse response of the differentiator using six-tap uniformly spaced. (Lower left) Impulse response of the differentiator using six-tap nonuniformly spaced. After [98].

microwave delay-line filter with nonuniformly spaced taps has been reported and experimentally demonstrated [98]. Fig. 19(left) shows the ideal response of a differentiator, while Fig. 19(a) displays the FIR of the required bandpass differentiator using uniformly spaced taps and Fig. 19(b) shows the FIR using nonuniformly spaced taps.

The six taps were generated using six wavelengths traveling through a dispersive fiber. The spectrum of the six-wavelength laser array is shown in Fig. 20(a). The measured magnitude and phase responses of the differentiator are shown in Fig. 20(b) and (c), respectively. The time delay has been chosen to obtain the center frequency of the passband filter at 9.95 GHz. The simulated magnitude and phase response of the six-tap FIR filter have been calculated using uniformly spaced taps generated with the coefficients shown in Fig. 19 (Lower right). To show reconfigurability of the differentiator a similar implementation has been done at the center frequency of 8.53 GHz. Fig. 20(d)–(f) shows the taps and the magnitude and phase responses of the differentiator.

A broadband incoherent light, previously filtered, is temporally modulated by the microwave signal to be transformed. The output is injected to a linear optical dispersive medium. In order to achieve the desired impulse response, the output from the dispersive medium is filtered with a dispersion-unbalanced optical interferometer as shown in the upper part of Fig. 21. A balanced detection scheme was used to cancel out the common background light. To validate the concept a real-time Fourier transformation (RTFT) of GHz-bandwidth microwave signals was implemented [100], including a square-like waveform, a sinusoidal pulse and a double pulse waveform.

Another example of application is connected to microwave radars where the pulses are usually phase-coded and a matched filter (correlator) is used to detect the signal. A nonuniformly spaced MWP delay-line filter has been proposed in for this application in [99].

An interesting field for the MWP application is the development devices performing a real time operations over microwave signals [100]–[103]. A first example is the Fourier transformation (RTFT) in the microwave region [100].

The lower part of Fig. 21 shows the experimental results for the RTFT of a sinusoid electrical pulse: The measured input

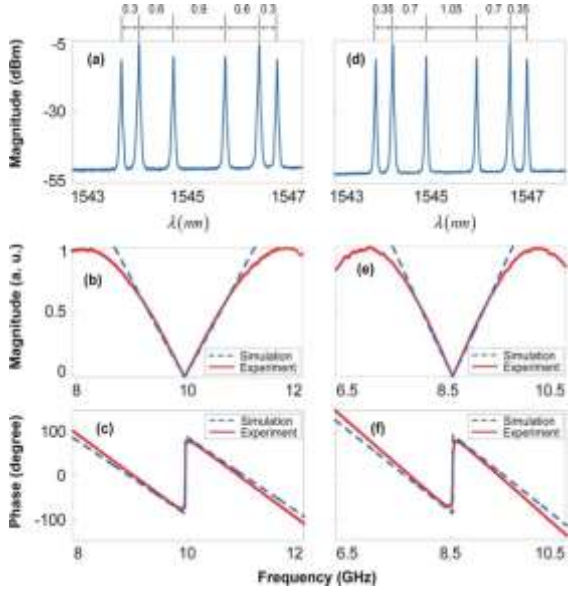

Fig. 20. (a) Measured spectrum of the six-wavelength laser array. Calculated (dashed) and measured (solid) (b) magnitude and (c) phase responses of the 9.95 GHz differentiator. (d) Measured spectrum of the six-wavelength laser array for the differentiator with a center frequency at 8.53 GHz. Calculated (dashed) and measured (solid). (e) Magnitude and (f) phase responses of the 8.53 GHz differentiator. After [98].

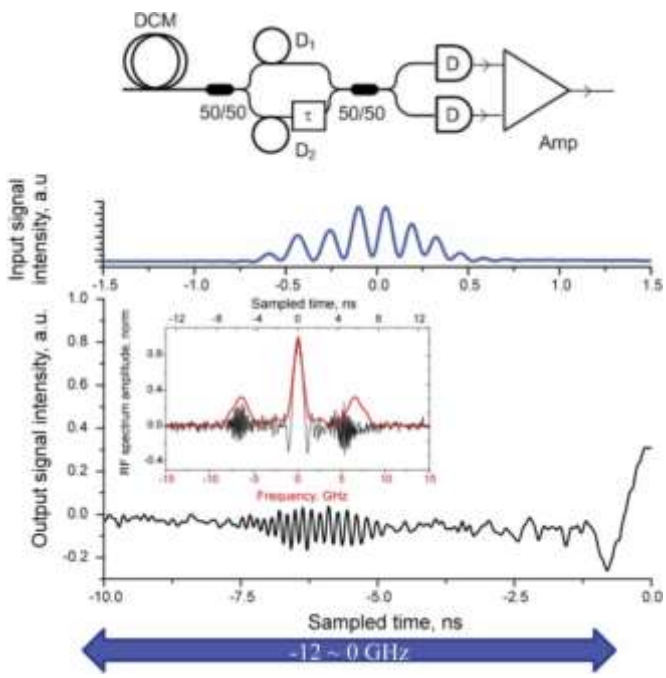

Fig. 21. (Upper) Schematic of the dispersion-unbalanced optical interferometer and the balanced detection scheme. (Lower) Experimental results for the RTFT of a sinusoid electrical pulse. After [100].

intensity waveform after light modulation, and the measured intensity waveform at the output of the created microwave dispersive filter. The measured waveform in full time scale is also shown in the inset together with the numerically calculated Fourier transform amplitude of the measured input time waveform. A second example is a method for ultrafast photonic time-intensity integration of an arbitrary microwave temporal waveform which has been demonstrated [101]. The

method is based on the superposition of mutually incoherent, continuously time-delayed replicas of the optical intensity waveform to be processed.

Finally, in connection to telecommunication applications, it is worth noticing a transceiver design based on the adaptation of a selective MWP filter by the incorporation of a tunable interferometric structure between the light source and a phase modulator. This transceiver offers the possibility to transmit and select SCM electrical signals in a frequency range established by the phase-to-intensity conversion response [104].

VI. Summary, Conclusions, and Future Directions

We have presented and reviewed the most significant advances in the field of MWP signal processing developed during the last years. Special attention has been paid to describe the novel techniques developed in order to overcome the major limitations of these subsystems under incoherent regime. The new and emergent field of integrated MWP filters has been presented and though still in its infancy, it is clearly an exciting future direction of research. The considerable development of this field during the period under review has crystalized as well in a number of novel application fields, both in the time and the frequency domain, some of which have been presented and reviewed as well. Next years will for sure witness novel efforts directed towards the implementation of a fully integrated MWP signal processor on a chipset. Novel materials and the exploitation of nonlinear effects in integrated waveguides will most probably enable future developments. This will, no doubt, open the way to new and cost-effective subsystems capable of supporting current application needs as well as future ones yet to be unveiled.

References

[1] J. Capmany and D. Novak, "Microwave photonics combines two worlds," *Nature Photon.*, vol. 1, pp. 319–330, 2007.
[2] J. P. Yao, "Microwave photonics," *J. Lightw. Technol.*, vol. 27, no. 3, pp. 314–335, Feb. 2009.
[3] A. J. Seeds and K. J. Williams, "Microwave photonics," *J. Lightw. Technol.*, vol. 24, no. 12, pp. 4628–4641, Dec. 2006.
[4] J. Capmany, B. Ortega, D. Pastor, and S. Sales, "Discrete-time optical processing of microwave signals," *J. Lightw. Technol.*, vol. 23, no. 2, pp. 702–723, Feb. 2005.
[5] J. Capmany, B. Ortega, and D. Pastor, "A tutorial on microwave photonic filters," *J. Lightw. Technol.*, vol. 24, no. 1, pp. 201–229, Jan. 2006.
[6] R. A. Minasian, "Photonic signal processing of microwave signals," *IEEE Trans. Microw. Theory Tech.*, vol. 54, no. 2, pp. 832–846, Feb. 2006.
[7] C. K. Madsen and J. H. Zhao, *Optical Filter Design and Analysis: A Signal Processing Approach*. New York: Wiley-Interscience, 1999.
[8] R. W. Boyd and D. J. Gauthier, "Controlling the velocity of light pulses," *Science*, vol. 326, pp. 1074–1077, 2009.
[9] A. Zadok, A. Eyal, and M. Tur, "Stimulated Brillouin scattering slow light in optical fibers," *Appl. Opt.*, vol. 50, pp. E38–E49, 2011.
[10] A. Loayssa and F. J. Lahoz, "Broad-band RF photonic phase-shifter based on stimulated Brillouin scattering and single-sideband modulation," *IEEE Photon. Technol. Lett.*, vol. 18, no. 1, pp. 208–210, Jan. 2006.
[11] A. Loayssa, J. Capmany, M. Sagues, and J. Mora, "Demonstration of incoherent microwave photonic filters with all-optical complex coefficients," *IEEE Photon. Technol. Lett.*, vol. 18, no. 16, pp. 1744–1746, Aug. 2006.
[12] M. Sagues, A. Loayssa, and J. Capmany, "Multitap complex-coefficient incoherent microwave photonic filters based on stimulated Brillouin scattering," *IEEE Photon. Technol. Lett.*, vol. 19, pp. 1194–1197, Aug. 2007.
[13] P. A. Morton and J. B. Khurgin, "Microwave photonic delay line with separate tuning of the optical carrier," *IEEE Photon. Technol. Lett.*, vol. 21, no. 22, pp. 1686–1688, Nov. 2009.
[14] J. Sancho, S. Chin, M. Sagues, A. Loayssa, J. Lloret, I. Gasulla, S. Sales, L. Thévenaz, and J. Capmany, "Dynamic microwave photonic filter using separate carrier tuning based on stimulated Brillouin scattering in fibers," *IEEE Photon. Technol. Lett.*, vol. 22, no. 23, pp. 1753–1755, Dec. 2010.
[15] S. Chin, L. Thévenaz, J. Sancho, S. Sales, J. Capmany, P. Berger, J. Bourderionnet, and D. Dolfi, "Broadband true time delay for microwave signal processing, using slow light based on stimulated Brillouin scattering in optical fibers," *Opt. Exp.*, vol. 18, pp. 22599–22613, 2010.
[16] K. Y. Song, W. Zou, Z. He, and K. Hotate, "All-optical dynamic grating generation based on Brillouin scattering in polarization-maintaining fiber," *Opt. Lett.*, vol. 33, pp. 926–928, 2008.
[17] J. Sancho, N. Primerov, S. Chin, Y. Antman, A. Zadok, S. Sales, and L. Thévenaz, "Tunable and reconfigurable multi-tap microwave photonic filter based on dynamic Brillouin gratings in fibers," *Opt. Exp.*, vol. 20, pp. 6157–6162, 2012.
[18] M. Sagues, R. G. Olcina, A. Loayssa, S. Sales, and J. Capmany, "Multi-tap complex-coefficient incoherent microwave photonic filters based on optical single-sideband modulation and narrow band optical filtering," *Opt. Exp.*, vol. 16, pp. 295–303, 2008.
[19] Y. Dai and J. P. Yao, "Nonuniformly-spaced photonic microwave delay-line filter," *Opt. Exp.*, vol. 16, no. 7, pp. 4713–4718, 2008.
[20] S. Sales, W. Xue, J. Mork, and I. Gasulla, "Slow and fast light effects and their applications to microwave photonics using semiconductor optical amplifiers," *IEEE Trans. Microw. Theory and Tech.*, vol. 58, no. 11, pp. 3022–3038, Nov. 2010.
[21] F. Ohman, K. Yvind, and J. Mork, "Slow light in a semiconductor waveguide for true-time delay applications in microwave photonics," *IEEE Photon. Technol. Lett.*, vol. 19, no. 15, pp. 1145–1147, Aug. 2007.
[22] W. Xue, Y. Chen, F. Öhman, S. Sales, and J. Mørk, "Enhancing light slow-down in semiconductor optical amplifiers by optical filtering," *Opt. Lett.*, vol. 33, pp. 1084–1086, 2008.
[23] W. Xue, S. Sales, J. Capmany, and J. Mørk, "Microwave phase shifter with controllable power response based on slow- and fast-light effects in semiconductor optical amplifiers," *Opt. Lett.*, vol. 34, pp. 929–931, 2009.
[24] W. Xue, S. Sales, J. Capmany, and J. Mørk, "Wideband 360θ microwave photonic phase shifter based on slow light in semiconductor optical amplifiers," *Opt. Exp.*, vol. 18, pp. 6156–6163, 2010.
[25] J. Sancho, J. Lloret, I. Gasulla, S. Sales, and J. Capmany, "Fully tunable 360° microwave photonic phase shifter based on a single semiconductor optical amplifier," *Opt. Exp.*, vol. 19, pp. 17421–17426, 2011.
[26] W. Xue, S. Sales, J. Mork, and J. Capmany, "Widely tunable microwave photonic notch filter based on slow and fast light effects," *IEEE Photon. Technol. Lett.*, vol. 21, no. 3, pp. 167–169, Feb. 2009.
[27] Y. Yan and J. P. Yao, "A tunable photonic microwave filter with a complex coefficient using an optical RF phase shifter," *IEEE Photon. Technol. Lett.*, vol. 19, no. 19, pp. 1472–1474, Oct. 2007.
[28] X. Yi, T. X. H. Huang, and R. A. Minasian, "Tunable and reconfigurable photonic signal processor with programmable all-optical complex coefficients," *IEEE Trans. Microw. Theory Tech. (Special Issue Microw. Photon.)*, vol. 58, no. 11, pp. 3088–3093, Nov. 2010.
[29] M. H. Song, V. Torres-Company, R. Wu, E. Hamidi, and A. M. Weiner, "Programmable multi-tap microwave photonic phase filtering via optical frequency comb shaping," in *Proc. Int. Topical Meet. Microw. Photon. Conf.*, Oct. 18–21, 2011, pp. 37–40.
[30] F. Zeng, J. Wang, and J. P. Yao, "All-optical microwave bandpass filter with negative coefficients based on a phase modulator and linearly chirped fiber Bragg gratings," *Opt. Lett.*, vol. 30, no. 17, pp. 2203–2205, Sep. 2005.

ISSN: 2278-4632
Vol-12 Issue-07 No.03 July 2022

[31] J. Wang, F. Zeng, and J. P. Yao, "All-optical microwave bandpass filter with negative coefficients based on PM-IM conversion," *IEEE Photon. Technol. Lett.*, vol. 17, no. 10, pp. 2176–2178, Oct. 2005.
[32] J. Mora, J. Capmany, A. Loayssa, and D. Pastor, "Novel technique for implementing incoherent microwave photonic filters with negative coefficients using phase modulation and single sideband selection," *IEEE Photon. Technol. Lett.*, vol. 18, no. 18, pp. 1943–1945, Sep. 2006.
[33] J. P. Yao and Q. Wang, "Photonic microwave bandpass filter with negative coefficients using a polarization modulator," *IEEE Photon. Technol. Lett.*, vol. 19, no. 9, pp. 644–646, May 2007.
[34] Q. Wang and J. P. Yao, "Multitap photonic microwave filters with arbitrary positive and negative coefficients using a polarization modulator and an optical polarizer," *IEEE Photon. Technol. Lett.*, vol. 20, no. 2, pp. 78–80, Jan. 2008.
[35] S.-C. Chan, Q. Liu, Z. Wang, and K. S. Chiang, "Tunable negative-tap photonic microwave filter based on a cladding-mode coupler and an optically injected laser of large detuning," *Opt. Exp.*, vol. 19, pp. 12045–12052, 2011.
[36] T. Chen, X. Yi, T. X. H. Huang, and R. A. Minasian, "Mul- tiple-bipolar-tap tunable spectrum sliced microwave photonic filter," *Opt. Lett.*, vol. 35, pp. 3934–3936, 2010.
[37] T. X. H. Huang, X. Yi, and R. A. Minasian, "Microwave photonic filters with programmable bipolar coefficients based on π-phase inversion of DSB sidebands," *Electron. Lett.*, vol. 46, pp. 1609–1610, 2010.
[38] M. D. Manzanedo, J. Mora, and J. Capmany, "Continuously tunable microwave photonic filter with negative coefficients using cross-phase modulation in an SOA-MZ interferometer," *IEEE Photon. Technol. Lett.*, vol. 20, no. 7, pp. 526–528, Apr. 2008.
[39] J. Mora, B. Ortega, A. Díez, J. L. Cruz, M. V. Andrés, J. Capmany, and D. Pastor, "Photonic microwave tunable single bandpass filter based on a Mach-Zehnder interferometer," *J. Lightw. Technol.*, vol. 24, no. 7, pp. 2500–2509, Jul. 2006.
[40] J. Mora, L. R. Chen, and J. Capmany, "Single bandpass microwave photonic filter with tuning and reconfiguration capabilities," *J. Lightw. Technol.*, vol. 26, no. 15, pp. 2663–2670, Aug. 2008.
[41] T. X. H. Huang, X. Yi, and R. A. Minasian, "Single passband microwave photonic filter using continuous-time impulse response," *Opt. Exp.*, vol. 19, pp. 6231–6242, 2011.
[42] J. Capmany, "On the cascade of incoherent discrete-time microwave photonic filters," *J. Lightw. Technol.*, vol. 24, no. 7, pp. 2564–2578, Jul. 2006.
[43] J. Palaci, G. E. Villanueva, J. V. Galan, J. Marti, and B. Vidal, "Single bandpass photonic microwave filter based on a notch ring resonator," *IEEE Photon. Technol. Lett.*, vol. 22, no. 17, pp. 1276–1278, Sep. 2010.
[44] J. Palací, P. Pérez-Millán, G. E. Villanueva, J. L. Cruz, M. V. Andrés, J. Martí, and B. Vidal, "Tunable photonic microwave filter with single bandpass based on a phase-shifted fiber Bragg grating," *IEEE Photon. Technol. Lett.*, vol. 22, no. 19, pp. 1467–1469, Oct. 2010.
[45] W. Zhang and R. A. Minasian, "Widely tunable single-passband microwave photonic filter based on stimulated Brillouin scattering," *IEEE Photon. Technol. Lett.*, vol. 23, no. 23, pp. 1775–1777, Dec. 2011.
[46] E. H. W. Chan and R. A. Minasian, "Widely tunable, high-FSR, coherence-free microwave photonic notch filter," *J. Lightw. Technol.*, vol. 26, no. 8, pp. 922–927, Apr. 2008.
[47] E. H. W. Chan, "Suppression of coherent interference effect in an optical delay line signal processor using a single tone phase modulation technique," *IEEE Photon. Technol. Lett.*, vol. 21, no. 4, pp. 215–217, Feb. 2009.
[48] E. H. W. Chan and R. A. Minasian, "Novel coherence-free RF/microwave photonic bandpass filter," *IEEE Photon. Technol. Lett.*, vol. 21, no. 4, pp. 230–232, Feb. 2009.
[49] E. H. W. Chan and R. A. Minasian, "Coherence-free high-resolution RF/microwave photonic bandpass filter with high skirt selectivity and high stopband attenuation," *J. Lightw. Technol.*, vol. 28, no. 11, pp. 1646–1651, Jun. 2010.
[50] E. H. W. Chan, "Cascaded multiple infinite impulse response optical delay line signal processor without coherent interference," *J. Lightw. Technol.*, vol. 29, no. 9, pp. 1401–1406, May 2011.
[51] E. H. W. Chan and R. A. Minasian, "High-resolution tunable RF/microwave photonic notch filter with low-noise performance," *J. Lightw. Technol.*, vol. 29, no. 21, pp. 3304–3309, Nov. 2011.
[52] J. Capmany, J. Mora, B. Ortega, and D. Pastor, "High Q microwave photonic filter using a tuned modulator," *Opt. Lett.*, pp. 2291–2301, 2005.
[53] B. Ortega, J. Mora, J. Capmany, D. Pastor, and R. Garcia-Olcina, "Highly selective microwave photonic filters based on an active optical recirculating cavity and tuned modulator hybrid structure," *Electron. Lett.*, vol. 41, pp. 1133–1135, 2005.
[54] J. Mora, B. Ortega, and J. Capmany, "Accurate control of active recirculating structures for microwave photonics signal filtering," *J. Lightw. Technol.*, vol. 26, no. 12, pp. 1626–1631, Jun. 2008.
[55] J. Capmany, J. Mora, B. Ortega, and D. Pastor, "High-quality low-cost online-reconfigurable microwave photonic transversal filter with positive and negative coefficients," *IEEE Photon. Technol. Lett.*, vol. 17, no. 12, pp. 2730–2732, Dec. 2005.
[56] E. Hamidi, D. E. Leaird, and A. M. Weiner, "Tunable programmable microwave photonic filters based on an optical frequency comb," *IEEE Trans. Microw. Theory Tech.*, vol. 58, no. 11, pp. 3269–3278, Nov. 2010.
[57] M. Song, C. M. Long, E. Hamidi, R. Wu, V. Supradeepa, D. Seo, D. E. Leaird, and A. M. Weiner, "Flat-top microwave photonic filter based on optical frequency comb shaping," presented at the presented at the Conf. Lasers Electro-Opt., Baltimore, MD, 2011, Paper CThI5.
[58] M. H. Song, C. M. Long, R. Wu, D. Seo, D. E. Leaird, and A. M. Weiner, "Reconfigurable and tunable flat-top microwave photonic filters utilizing optical frequency comb," *IEEE Photon. Technol. Lett.*, vol. 23, no. 21, pp. 1618–1620, Nov. 2011.
[59] V. R. Supradeepa, C. M. Long, R. Wu, F. Ferdous, E. Hamidi, D. E. Leaird, and A. M. Weiner, "Comb-based radiofrequency photonic filters with rapid tunability and high selectivity," *Nature Photon.*, vol. 6, pp. 186–194, 2012.
[60] S. Xiao and A. M. Weiner, "Programmable photonic microwave filters with arbitrary ultra wideband phase response," *IEEE Trans. Microw. Theory Tech.*, vol. 54, no. 11, pp. 4002–4008, Nov. 2006.
[61] E. J. Norberg, R. S. Guzzon, S. C. Nicholes, J. S. Parker, and L. A. Coldren, "Programmable photonic lattice filters in InGaAsP-InP," *Photon. Technol. Lett.*, vol. 22, pp. 109–111, 2010.
[62] R. S. Guzzon, E. J. Norberg, J. S. Parker, L. A. Johansson, and L. A. Coldren, "Monolithically integrated programmable photonic microwave filter with tunable inter-ring coupling," in *Proc. IEEE Top. Meeting Microw. Photon.*, Montreal, QC, Canada, 2010, pp. 23–26.
[63] E. J. Norberg, R. S. Guzzon, J. S. Parker, L. A. Johansson, and L. A. Coldren, "A monolithic programmable optical filter for RF-signal processing," in *Proc. IEEE Top. Meeting Microw. Photon.*, Montreal, QC, Canada, 2010, pp. 365–368.
[64] E. J. Norberg, R. S. Guzzon, J. S. Parker, and L. A. Coldren, "Programmable photonic filters from monolithically cascaded filter stages," presented at the presented at the Proc. Integr. Photon. Res., Silicon Nanophoton., Monterey, CA, 2010, Paper ITuC3.
[65] E. J. Norberg, R. S. Guzzon, J. S. Parker, L. A. Johansson, and L. A. Coldren, "Programmable photonic microwave filters monolithically integrated in InP/InGaAsP," *J. Lightw. Technol.*, vol. 29, no. 11, pp. 1611–1619, Jun. 2011.
[66] R. S. Guzzon, E. J. Norberg, J. S. Parker, L. A. Johansson, and L. A. Coldren, "Integrated InP-InGaAsP tunable coupled ring optical bandpass filters with zero insertion loss," *Opt. Exp.*, vol. 19, pp. 7816–7826, 2011.
[67] H.-W. Chen, A. W. Fang, J. Bovington, J. Peters, and J. Bowers, "Hybridsilicon tunable filter based on a Mach-Zehnder interferometer and ring resonantor," in *Proc. Int. Top. Meeting Microw. Photon.*, Valencia, Spain, 2009, pp. 1–4.
[68] H.-W. Chen, A. W. Fang, J. D. Peters, Z. Wang, J. Bovington, D. Liang, and J. E. Bowers, "Integrated microwave photonic filter on a hybrid silicon platform," *IEEE Trans. Microw. Theory Tech.*, vol. 58, no. 11, pp. 3213–3219, Nov. 2010.
[69] P. Dong, N. N. Feng, D. Feng, W. Qian, H. Liang, D. C. Lee, B. J. Luff, T. Banwell, A. Agarwal, P. Toliver, R. Menendez, T. K. Woodward, and M. Asghari, "GHz-bandwidth optical filters based on high-order silicon ring resonators," *Opt. Exp.*, vol. 18, pp. 23784–23789, 2010.
[70] N. N. Feng, P. Dong, D. Feng, W. Qian, H. Liang, D. C. Lee, J. B. Luff, A. Agarwal, T. Banwell, R. Menendez, P. Toliver, T. K. Woodward, and M. Asghari, "Thermally-efficient reconfigurable narrowband RF-photonic filter," *Opt. Exp.*, vol. 18, pp. 24648–24653, 2010.
[71] M. Rasras, K. Tu, D. Gill, Y. Chen, A. White, S. Patel, A. Pomerene, D. Carothers, J. Beattie, M. Beals, J. Michel, and L. Kimerling, "Demonstration of a tunable microwave-photonic notch filter using low-loss silicon ring resonators," *J. Lightw. Technol.*, vol. 27, no. 12, pp. 2105–2110, Jun. 2009.

ISSN: 2278-4632
Vol-12 Issue-07 No.03 July 2022

[72] J. Lloret, J. Sancho, M. Pu, I. Gasulla, K. Yvind, S. Sales, and J. Capmany, "Tunable complex-valued multi-tap microwave photonic filter based on single silicon-on-insulator microring resonator," *Opt. Exp.*, vol. 19, pp. 12402–12407, 2011.
[73] J. Lloret, G. Morthier, F. Ramos, S. Sales, D. Van Thourhout, T. Spuesens, N. Olivier, J.-M. Fédéli, and J. Capmany, "Broadband microwave photonic fully tunable filter using a single heterogeneously integrated III-V/SOI-microdisk-based phase shifter," *Opt. Exp.*, vol. 20, pp. 10796–10806, 2012.
[74] D. Marpaung, C. Roeloffzen, A. Leinse, and M. Hoekman, "A photonic chip based frequency discriminator for a high performance microwave photonic link," *Opt. Exp.*, vol. 18, pp. 27359–27370, 2010.
[75] M. Burla, D. Marpaung, L. Zhuang, C. Roeloffzen, M. R. Khan, A. Leinse, M. Hoekman, and R. Heideman, "On-chip CMOS compatible reconfigurable optical delay line with separate carrier tuning for microwave photonic signal processing," *Opt. Exp.*, vol. 19, pp. 21475–21484, 2011.
[76] L. Zhuang, D. Marpaung, M. Burla, W. Beeker, A. Leinse, and C. Roeloffzen, "Low-loss, high-index-contrast Si_3N_4/SiO_2 optical waveguides for optical delay lines in microwave photonics signal processing," *Opt. Exp.*, vol. 19, pp. 23162–23170, 2011.
[77] J. Sancho, J. Bourderionnet, J. Lloret, S. Combrié, I. Gasulla, S. Xavier, S. Sales, P. Colman, G. Lehoucq, D. Dolfi, J. Capmany, and A. De Rossi, "Integrable microwave filter based on a photonic crystal delay line," *Nature Communications*, 3:1075 DOI:10.1038/ncomms2092 (2012).
[78] D. Marpaung, C. Roeloffzen, R. Heideman, A. Leinse, S. Sales, and J. Capmany, "Integrated microwave photonics," *Lasers Photon. Rev.*, to be published.
[79] C. H. Cox, III, *Analog Photonic Links: Theory and Practice*. Cambridge, U.K.: Cambridge Univ. Press, 2004.
[80] J. M. Wyrwas and M. C. Wu, "Dynamic range of frequency modulated direct-detection analog fiber optic links," *J. Lightw. Technol.*, vol. 27, no. 24, pp. 5552–5562, Dec. 2009.
[81] I. Gasulla and J. Capmany, "Analytical model and figures of merit for filtered microwave photonic links," *Opt. Exp.*, vol. 19, pp. 19758–19774, 2011.
[82] M. Rius, J. Mora, M. Bolea, and J. Capmany, "Harmonic distortion in microwave photonic filters," *Opt. Exp.*, vol. 20, pp. 8871–8876, 2012.
[83] M. Bolea, J. Mora, B. Ortega, and J. Capmany, "Optical UWB pulse generator using an N tap microwave photonic filter and phase inversion adaptable to different pulse modulation formats," *Opt. Exp.*, vol. 17, pp. 5023–5032, 2009.
[84] M. Bolea, J. Mora, B. Ortega, and J. Capmany, "Photonic arbitrary waveform generation applicable to multiband UWB communications," *Opt. Exp.*, vol. 18, pp. 26259–26267, 2010.
[85] M. Bolea, J. Mora, B. Ortega, and J. Capmany, "Flexible monocycle UWB generation for reconfigurable access networks," *IEEE Photon. Technol. Lett.*, vol. 22, no. 12, pp. 878–880, Jun. 2010.
[86] H. Mu and J. P. Yao, "Polarity- and shape-switchable UWB pulse generation based on a photonic microwave delay-line filter with a negative tap coefficient," *IEEE Photon. Technol. Lett.*, vol. 21, no. 17, pp. 1253–1255, Sep. 2009.
[87] S. Pan and J. P. Yao, "Optical generation of polarity- and shape-switchable UWB pulses using a chirped intensity modulator and a first-order asymmetric Mach-Zehnder interferometer," *Opt. Lett.*, vol. 34, pp. 1312–1314, 2009.
[88] S. Pan and J. P. Yao, "Switchable UWB pulses generation using a phase modulator and a reconfigurable asymmetric Mach-Zehnder interferometer," *Opt. Lett.*, vol. 34, pp. 160–162, 2009.
[89] E. Hamidi and A. M. Weiner, "Phase-only matched filtering of ultrawideband arbitrary microwave waveforms via optical pulse shaping," *J. Lightw. Technol.*, vol. 26, no. 15, pp. 2355–2363, Aug. 2008.
[90] M. Kahn, H. Shen, Y. Xuan, L. Zhao, S. Xiao, D. Leaird, A. Weiner, and M. Qi, "Ultrabroad-bandwidth arbitrary radiofrequency waveform generation with a silicon photonic chip-based spectral shaper," *Nature Photon.*, vol. 4, pp. 117–122, 2009.
[91] M. Bolea, J. Mora, B. Ortega, and J. Capmany, "Optical arbitrary waveform generator using incoherent microwave photonic filtering," *IEEE Photon. Technol. Lett.*, vol. 23, no. 10, pp. 618–620, May 2011.
[92] J. P. Yao, "Photonic generation of microwave arbitrary waveforms," *Opt. Commun.*, vol. 284, pp. 3723–3736, Jul. 2011.
[93] Z. Li, Y. Han, H. Chi, X. Zhang, and J. P. Yao, "A continuously tunable microwave fractional Hilbert transformer based on a nonuniformly-spaced photonic microwave delay-line filter," *J. Lightw. Technol.*, vol. 30, no. 12, pp. 1948–1953, Jun. 2012.
[94] C. Wang and J. P. Yao, "Chirped microwave pulse compression using a photonic microwave filter with a nonlinear phase response," *IEEE Trans. Microw. Theory Tech.*, vol. 57, no. 2, pp. 496–504, Feb. 2009.
[95] Y. Dai and J. P. Yao, "Chirped microwave pulse generation using a photonic microwave delay-line filter with a quadratic phase response," *IEEE Photon. Technol. Lett.*, vol. 21, no. 9, pp. 569–571, May 2009.
[96] M. Bolea, J. Mora, B. Ortega, and J. Capmany, "Nonlinear dispersion-based incoherent photonic processing for microwave pulse generation with full reconfigurability," *Opt. Exp.*, vol. 20, pp. 6278–6736, 2012.
[97] E. Hamidi and A. M. Weiner, "Post-compensation of ultra-wideband antenna dispersion using microwave photonic phase filters and its applications to UWB systems," *IEEE Trans. Microw. Theory Tech.*, vol. 57, no. 4, pp. 890–898, Apr. 2009.
[98] Y. Han, Z. Li, and J. P. Yao, "A microwave bandpass differentiator implemented based on a nonuniformly-spaced photonic microwave delay-line filter," *J. Lightw. Technol.*, vol. 29, no. 22, pp. 3470–3475, Nov. 2011.
[99] Y. Dai and J. P. Yao, "Microwave correlator based on a nonuniformly spaced photonic microwave delay-line filter," *IEEE Photon. Technol. Lett.*, vol. 21, no. 14, pp. 969–971, Jul. 2009.
[100] Y. Park, M. H. Asghari, R. Helsten, and J. Azaña, "Implementation of broadband microwave arbitrary-order time differential operators using a reconfigurable incoherent photonic processor," *IEEE Photon. J.*, vol. 2, no. 6, pp. 1040–1050, Dec. 2010.
[101] M. H. Asghari, Y. Park, and J. Azaña, "Photonic temporal integration of broadband microwave waveforms over nanosecond time windows," presented at the presented at the Signal Process. Photon. Commun. Conf., Toronto, ON, Canada, Paper SPWD1.
[102] Y. Park and J. Azaña, "Optical signal processors based on a time-spectrum convolution," *Opt. Lett.*, vol. 35, pp. 796–798, 2010.
[103] Y. Park and J. Azaña, "Ultrahigh dispersion of broadband microwave signals by incoherent photonic processing," *Opt. Exp.*, vol. 18, pp. 14752–14761, 2010.
[104] F. Grassi, J. Mora, B. Ortega, and J. Capmany, "Radio over fiber transceiver employing phase modulation of an optical broadband source," *Opt. Exp.*, vol. 18, pp. 21750–21756, 2010.